Batteries & Supercaps

Review
doi.org/10.1002/batt.202400284

Chemistry Europe
European Chemical Societies Publishing

www.batteries-supercaps.org

Challenges and Prospects of Electrolyte Design for Lithium-Sulfurized Polyacrylonitrile Batteries

Tao Ma[a, b] and Zhanliang Tao*[a]

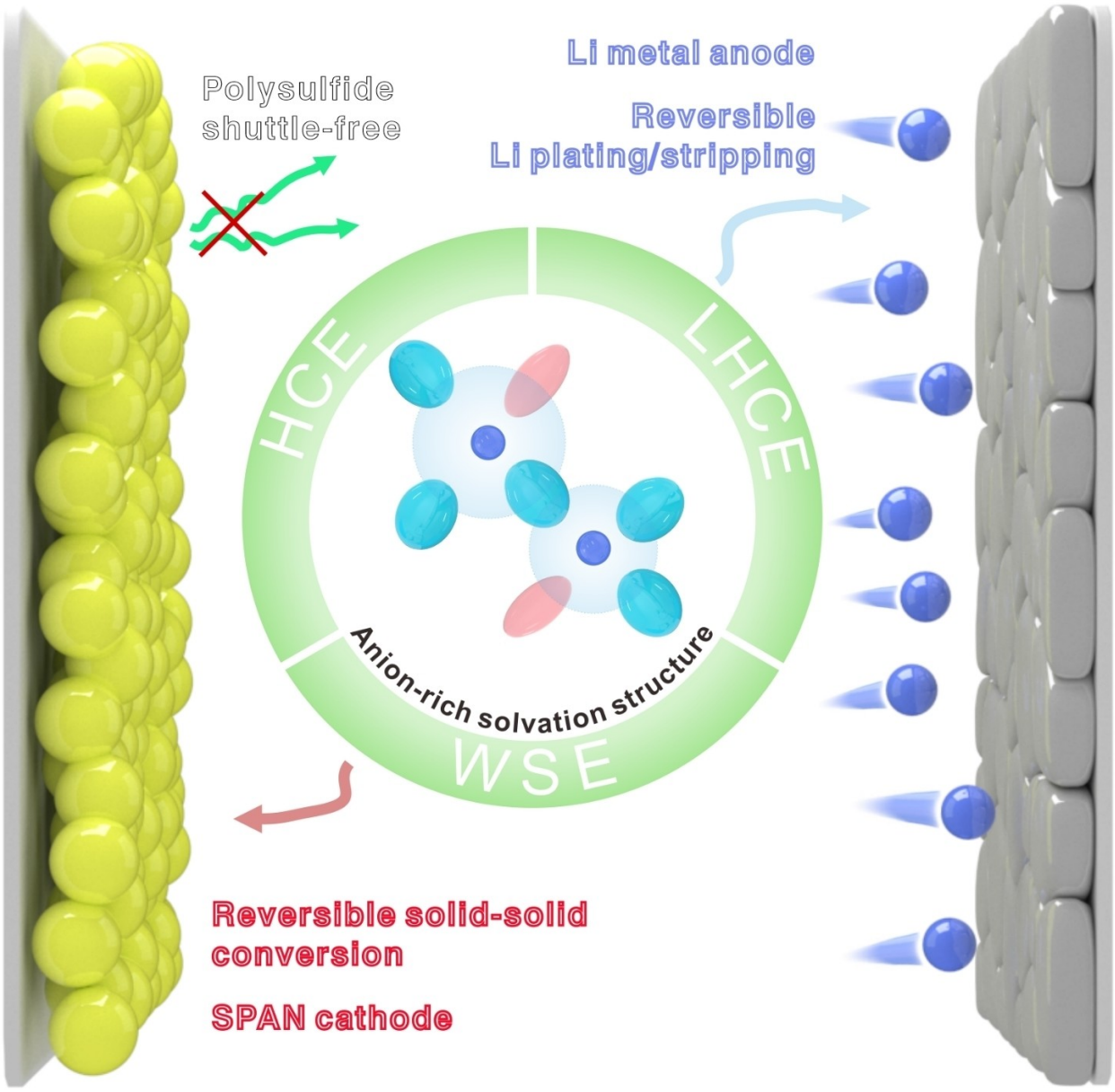

Sulfurized polyacrylonitrile (SPAN) is regarded as a promising organic sulphur cathode material for lithium-sulfur (Li–S) batteries. It undergoes a solid-solid conversion without forming polysulfide intermediate phases, overcoming the poor electrochemical performance caused by the shuttle effect of elemental S cathodes. However, realizing this unique conversion mechanism requires employing appropriate electrolytes. Furthermore, the direct application of metallic Li as the anode unavoidable introduces a series of issues triggered by Li dendrites in Li-SPAN batteries, such as low lifespan, short circuits, fire, etc. In this review, we endeavor to encapsulate recent advancements in electrolyte research, with a particular focus on the intrinsic relationship between the solvation structure of the electrolyte and the interfacial chemistry of the Li anode and SPAN electrode, aim to provide insights into the electrolytes design for high performance Li-SPAN full batteries.

1. Introduction

Since first commercialization in 1991, lithium (Li) ion batteries (LIBs), characterized by their high energy density, extended cycle life, and compact size, have emerged as the preferred power source for portable devices such as mobile phones and laptops.[1–3] Entering the new century, motivated by the pursuit of a low-carbon lifestyle, LIBs began to supplant traditional internal combustion engines, serving as a vital power source for vehicles.[4] In recent years, with the continuous evolution of the electric vehicle (EV) industry, the issue of range anxiety has been raised. However, the energy density of conventional LIBs is approaching its theoretical limit, thus underscoring the pressing need to develop high energy density battery systems.[5] From the standpoint of electrochemistry, the materials based on multi-electron reactions constitute the cornerstone for the construction of high energy density Li secondary batteries. Sulfur (S), based on a 16-electron transfer reaction, exhibits an extraordinarily high theoretical specific capacity (1675 $mAh\,g^{-1}$). When combined with Li metal, the theoretical energy density of the Li–S batteries can ascend to as much as 2600 $Wh\,kg^{-1}$, far surpassing that of existing LIBs.[6,7] Additionally, S is abundant in nature and characterized by its low cost and environmental friendliness.[8,9] Overall, high energy density Li–S batteries hold the potential to alleviate range anxiety considerably, meeting the demands for extended range in drones and EVs, while also satisfying the pursuit of low-cost cells in the field of large-scale energy storage.

The key to realizing high specific energy Li–S batteries lies in the development of high performance S cathodes. Elemental S and sulfurized polyacrylonitrile (SPAN) are principal sulfur-based cathode materials, each following distinctly different reaction mechanisms.[10–12] Elemental S undergoes a two-phase redox conversion reaction in ether electrolyte.[12,13] During the discharge process, solid-phase S_8 is initially converted into soluble long-chain polysulfides (Li_2S_x, $4 \leq x \leq 8$), which then further reduce to short-chain polysulfides (Li_2S_x, $2 \leq x \leq 4$), ultimately depositing as solid discharge products Li_2S_2/Li_2S onto the conductive substrate. In the charging process, the discharge products continuously lose electrons, transforming short-chain polysulfides and long-chain polysulfides, ultimately reverting to S_8.[10,11] As the charging/discharging process involves a solid-liquid phase conversion, it unavoidably leads to polysulfide dissolution. The polysulfides dissolved in the electrolyte can cause a shuttle effect, where, driven by the concentration field, polysulfides cross the separator to reach the Li metal side. This results in the loss of active materials and corrosion of the Li metal anode, leading to premature battery failure.[14–16]

Unlike elemental S, SPAN demonstrates a solid-solid conversion in conventional ester-based electrolytes, effectively addressing the challenges of low coulombic efficiency (CE), limited cycle life, and rapid capacity decay typically associated with the shuttle effect in traditional elemental S cathodes.[17–21] Due to the absence of liquid phase conversion processes, there is no limitation on the amount of electrolyte used, allowing the SPAN cathode to operate normally under lean electrolyte conditions. Additionally, owing to the presence of a polypyrrole conductive framework, SPAN (10^{-5} to 10^{-7} $S\,cm^{-1}$)[22] exhibits remarkable conductivity compared to elemental S (10^{-30} $S\,cm^{-1}$),[23] obviating the need for significant additional conductive carbon during electrode fabrication. However, due to the inherent structural constraints of the polypyridine conductive framework, SPAN suffers from the drawback of a low sulfur content, which is limited to 56 wt%.[24–26] Other challenges lie in the retarded redox kinetics. Although the solid-solid conversion mechanism offers unique stability advantages (polysulfide-free), it also requires higher energy input and a longer time to complete, resulting in relatively slow conversion kinetics.[24,27] Even so, the unique polysulfide-free conversion mechanism makes SPAN considered a more commercially viable cathode material for Li–S batteries.

Notably, another significant challenge faced by Li–S batteries arises from the Li metal anode. Li metal is a double-edged sword, as the "holy grail" of anode materials, it possesses an extremely high theoretical specific capacity (3860 $mAh\,g^{-1}$) and low oxidation potential (−3.04 V vs. the standard hydrogen electrode).[28] However, its inherent chemical reactivity and uncontrollable deposition behavior lead to a series of issues. When the Li metal anode comes into contact with the electrolyte, a solid electrolyte interphase (SEI) film spontaneously forms.[33–35] This film possesses ionic conductivity while being electronically insulating, which protects the Li metal anode from continuous chemical reactions.[36] However, during prolonged cycling, factors such as volume changes, mechanical stress, dendrite growth, and high temperatures cause the SEI

[a] T. Ma, Z. Tao
Key Laboratory of Advanced Energy Materials Chemistry (Ministry of Education), College of Chemistry, State Key Laboratory of Advanced Chemical Power Sources, Collaborative Innovation Center of Chemical Science and Engineering (Tianjin), Nankai University, Tianjin 300071, China
E-mail: taozhl@nankai.edu.cn
[b] T. Ma
Battery Research Institute, Engineering R&D Institute, Hefei Gotion High-tech Power Energy Co., Ltd, Hefei 230012, China

film to undergo continuous breakage and repair, resulting in the irreversible consumption of active Li.[37] Furthermore, the deposition/stripping processes of Li cannot achieve 100% conversion. During stripping, some Li converts into electronically insulating Li (known as "dead Li"), which cannot participate in subsequent electrochemical processes.[38] The formation of dead Li and the continuous regeneration of the SEI film consume active Li, significantly reducing the lifespan of Li–S batteries. What's worse, Li plating may induce Li dendrite formation under the influence of factors such as tip effects, concentration gradients, and mechanical stress, leading to battery short circuits and safety concerns.[39–42] In contrast, ether-based electrolytes demonstrate enhanced chemical compatibility with the Li metal anode, offering superior safety and reversibility compared to ester-based electrolytes.[43–45] Regrettably, the operation of SPAN in conventional ether-based electrolytes is accompanied by the dissolution of polysulfides, triggering a swift deterioration in the electrochemical performance.[17,46,47]

As an essential component, the electrolyte not only influences the conversion process of SPAN but also impacts the cyclic reversibility of the Li metal anode. While certain electrolyte formulations may exhibit excellent reversibility with either the Li metal or SPAN cathode individually, they may not necessarily be compatible with both components simultaneously. This electrochemical incompatibility can lead to premature battery failure, such as dendrite formation on the Li anode or degradation of the SPAN cathode material. To address this challenge, researchers have been actively exploring various electrolyte compositions and additives that can enhance the stability and performance of Li-SPAN full batteries. In this review, we are dedicated to offering comprehensive commentary remarks on recent studies on electrolytes about Li-SPAN batteries. We meticulously analyze the impact of electrolytes on both the SPAN cathode and Li metal anode, aiming to provide insights for designing high performance electrolytes for Li-SPAN batteries.

2. Impact of Electrolyte on the SPAN Cathode

SPAN is often considered to undergo one-step solid-solid conversion without the formation of intermediate products (polysulfides) (Figure 1a), but this assumption is based on the use of suitable electrolytes.[17,48] SPAN follows distinctly different conversion mechanisms in various types of electrolytes, primarily depending on the abilities of electrolytes to inhibit polysulfides. During the discharge process, SPAN undergoes lithiation along with the reductive decomposition of solvents, Li salts, and additives.[48] Electrolytes with different solvation chemistry enable endow SPAN interface different structures and compositions. An excellent cathode electrolyte interphase (CEI) layer can encapsulate the SPAN material, preventing the dissolution of polysulfides into the electrolyte, thereby spatially constraining the electrochemical reactions and resulting in reversible solid-solid conversion.[29,49] Additionally, the solubility of polysulfides in the electrolyte is also a contributing factor. In contrast, polysulfides in electrolytes with high-polarity solvents are associated with serious polysulfide dissolution, leading to worse electrochemistry performance.[50,51]

2.1. Ester Electrolyte

Early research on SPAN primarily focused on material synthesis and modification. In these experiments, the conventional Li-ion battery electrolyte formula was prevalent, involving the dissolution of lithium hexafluorophosphate ($LiPF_6$) in a hybrid solvent blend of ethylene carbonate (EC), and linear carbonates, specifically dimethyl carbonate (DMC), diethyl carbonate (DEC), and ethyl methyl carbonate (EMC).[52–54] In routine ester-based electrolytes, SPAN undergoes reversible solid-solid conversion, demonstrating excellent cyclic stability.

Shen et al. discovered that not all ester-based electrolytes are compatible with SPAN cathode, a feasibility realized only in the presence of EC solvent in the electrolyte.[29] Further research demonstrated that cyclic EC decomposes to form a CEI layer containing polycarbonates, which effectively inhibits the dissolution of polysulfides into the electrolyte during the charge/discharge processes (Figure 1b). Building on this finding, the author tailored a 2 M electrolyte for Li-SPAN cells that simultaneously ensures the stability of both the Li anode and SPAN cathode by utilizing EC as the sole solvent and lithium bis(fluorosulfonyl)imide (LiFSI) as the Li salt. Yang et al. investigated the impact of cyclic ester solvents, including EC, vinylene carbonate (VC), and fluoroethylene carbonate (FEC), on the performance of the SPAN cathode.[30] The results indicated that SPAN exhibited the most favorable electrochemical performance in an electrolyte where FEC was used as a co-solvent. Subsequent investigations revealed that FEC demon-

Tao Ma is currently a R&D engineer in Hefei Gotion High-tech Power Energy Co., Ltd. He received his Ph.D. from College of Chemistry at Nankai University in 2024. His current research interests lie in electrolyte design and electrode structure optimization for high energy density cell, with a focus on solvation regulation and interfacial chemistry.

Zhanliang Tao is currently a professor in College of Chemistry at Nankai University. His research interests include synthesis of organic cathode materials, the design of low temperature aqueous zinc electrolytes, and the protection of zinc metal anode.

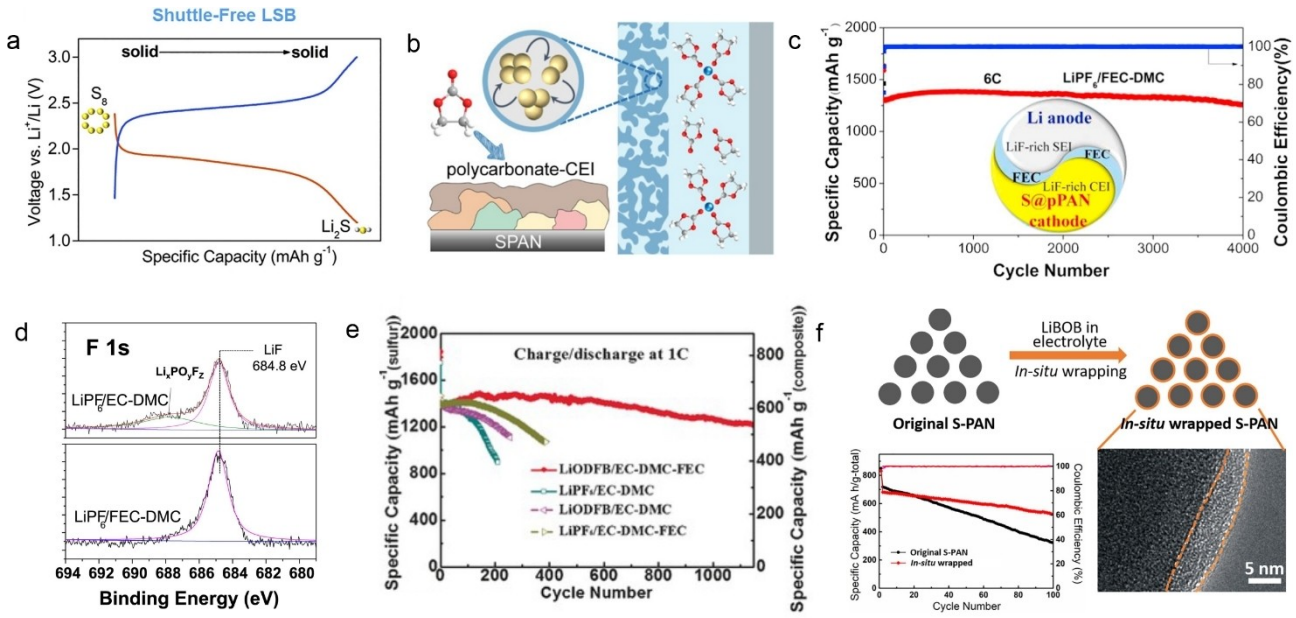

Figure 1. a) Voltage-capacity curve of Li-SPAN cell based on solid-solid conversion mechanism. Reproduced from ref. [17] Copyright (2023), with permission from Elsevier. b) Schematic diagram of the effect of EC for SPAN cathode. Reproduced from ref. [29] Copyright (2021), with permission from American Chemical Society. c) Long-term cycle performance of Li-SPAN cell in FEC-based electrolyte, d) X-ray photoelectron spectroscopy spectra of SPAN cathodes after cycling in different electrolytes. Reproduced from ref. [30] Copyright (2018), with permission from Elsevier. e) Long-term cycle performance of Li-SPAN cells in different electrolytes. Reproduced from ref. [31] Copyright (2016), with Wiley-VCH. f) Effect of LiBOB on SPAN cathodes cycle performance and interfacial chemistry.Reproduced from ref. [32] Copyright (2019), with permission from Elsevier.

strated optimal film-forming characteristics, leading to an increase in the content of lithium fluoride (LiF) in the CEI layer (Figure 1d). This effectively mitigated the volume expansion of SPAN and minimized potential electrolyte attacks. The incorporation of FEC led to the remarkable achievement of over 4000 cycles at a 6 C rate in the Li-SPAN cells (Figure 1c).

In addition to $LiPF_6$ and LiFSI, lithium bis(oxalato)borate (LiBOB) and lithium oxalyldifluoroborate (LiODFB) were also investigated as Li salts in electrolytes for Li-SPAN batteries. Unlike conventional Li salts, LiBOB and LiODFB are commonly used film-forming additives in LIBs that can effectively improve electrode interfacial behavior.[58] Xu et al. substituted $LiPF_6$ with LiODFB as the Li salt and combined routine ester solvents to form the electrolyte, enabling Li-SPAN batteries to exhibit better cycle performance, with capacity retention of 89% after 1100 cycles (Figure 1e). Further studies revealed that LiODFB contributes to CEI formation, enhancing interface stability and suppressing side reactions.[31] Jin et al. significantly improved the long cycle stability of the Li-SPAN battery by adding a small amount (0.5–2 wt%) LiBOB as an additive in conventional ester electrolytes.[32] Further research on the electrode interface revealed that LiBOB played a role in the CEI formation, and the resulting products effectively prevented side reactions between the electrolyte and the SPAN cathode (Figure 1f).

2.2. Ether Electrolyte

Despite ester-based electrolytes exhibiting well electrochemical stability for SPAN cathode, their chemical incompatibility with the Li metal anode limits the lifespan of Li-SPAN full cells.[29,57,59] In contrast, ether solvents offer higher chemical stability and reversibility towards Li metal. However, when SPAN operates in ether-based electrolytes (using high solvating power solvents), it typically accompanies a solid-liquid conversion process.[17,46] This occurs because, in highly solvating electrolytes, solvent molecules dominate the solvation structure and cannot form a stable CEI layer on the SPAN surface. During the operation of Li-SPAN batteries, polysulfides can leach out from cracks in the CEI layer, leading to the loss of active materials and subsequent deterioration in battery performance.[48,55]

Lithium nitrate ($LiNO_3$) is a regularly ester-based electrolyte additive in Li–S batteries that employs elemental S as a cathode, serving to protect the Li metal anode from polysulfide corrosion and acting as an ideal overcharge inhibitor.[60,61] Related research has revealed that $LiNO_3$ also plays a protective role in Li-SPAN batteries.[56,62] It participates in the formation of CEI layers on the SPAN cathode, effectively preventing charge/discharge by-products (polysulfides) from dissolving into the electrolyte (Figure 2a), thereby leading to improved electrochemical performance.[55] However, ether solvents encounter challenges in breaking the electrostatic interaction between anions and cations in $LiNO_3$. Typically, only highly solvation power ether solvents, such as diglyme, 1,2-dimethoxyethane (DME), 1,3-dioxolane, etc. can extensively dissolve $LiNO_3$.[63–65] This requirement, in effect, limits its application range. To overcome this barrier, Holoubek et al. introduced $LiNO_3$ during the slurry preparation process and obtained a SPAN electrode containing $LiNO_3$ particles.[56] During subsequent cycles, $LiNO_3$ continuously leaches out from the electrode and releases into

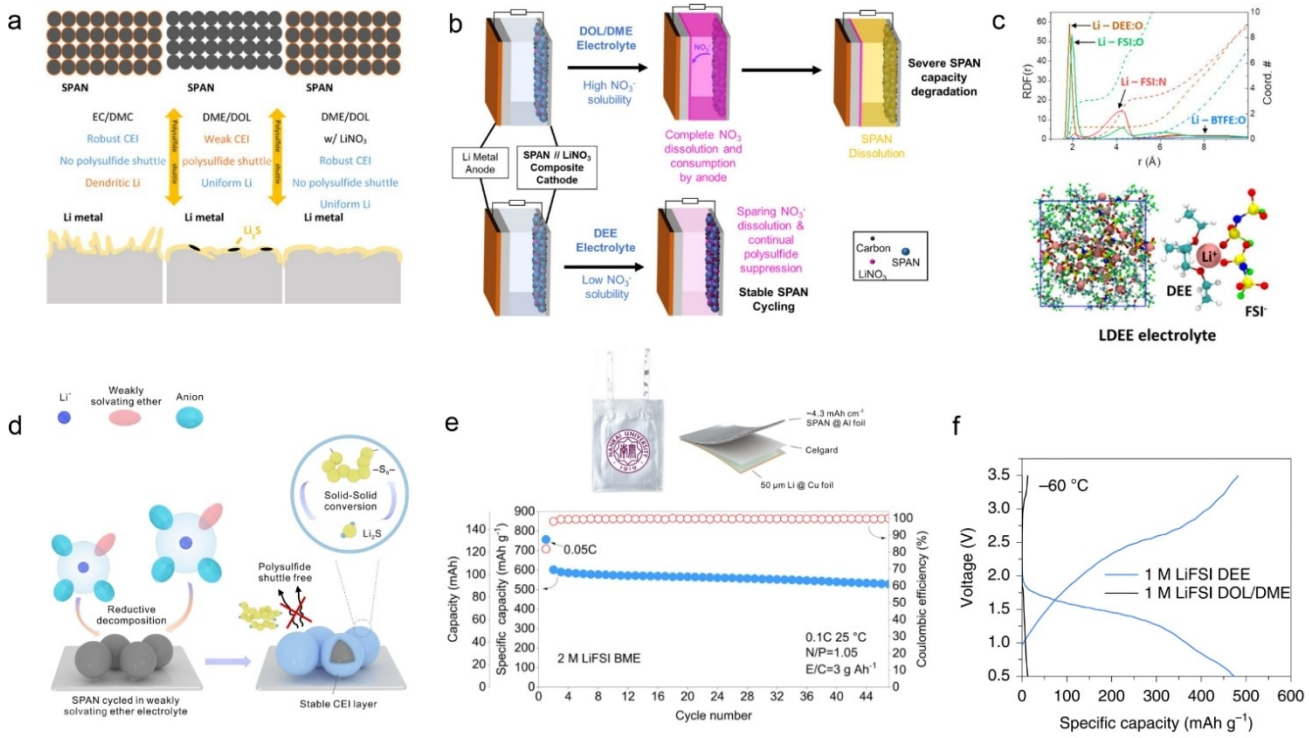

Figure 2. a) Effects of different electrolytes on the CEI layer of SPAN and SEI layer of Li metal. Reproduced from ref. [55] Copyright (2021), with permission from American Chemical Society. b) Working schematic of the $LiNO_3$/SPAN composite cathode. Reproduced from ref. [56] Copyright (2021), with permission from American Chemical Society. c) Radial distribution function, snapshot, and solvation structure of 1.8 M LiFSI DEE BTFE electrolyte obtained by molecular dynamics simulation. Reproduced from ref. [57] Copyright (2021), with permission from Elsevier. d) Effect of weakly solvating ether electrolyte on SPAN conversion reaction. e) Cycle performance of Li-SPAN pouch cell employs 2 M LiFSI BME electrolyte. Reproduced from ref. [48] Copyright (2023), with Wiley-VCH. f) Voltage-capacity curve of the Li-SPAN cells employs different electrolytes at −60 °C. Reproduced from ref. [51] Copyright (2021), with permission from Springer Nature.

the electrolyte. This method enables $LiNO_3$ to stabilize the SPAN cathode, even if low-polarity diethyl ether (DEE) is used as an electrolyte solvent (Figure 2b).

Research on $LiNO_3$ contributes significantly to understanding the crucial role of the CEI layer for SPAN. Anions, essential as components in the electrolyte, also possess film-forming properties. Their film-forming ability is directly related to the electrolyte composition, and as the electrolyte concentration increases, the stability of the CEI layer also improves.[66,67] Liu et al. have introduced a localized high concentration electrolyte (LHCE), employing LiFSI as the Li salt, low solvation power solvent DEE as the solvent, and 2,2,2-trifluoroethyl ether (BTFE) as a diluent.[57] Within the electrolyte (1.8 M LiFSI DEE BTFE), an abundant Li^+-FSI^- ion pair can be observed (Figure 2c), which facilitates the creation of a LiF-rich CEI layer on SPAN. This layer inhibits the dissolution of intermediate products during the charge/discharge process, enabling Li-SPAN cells to exhibit over 1200 stable cycles. Conversely, the CEI layer derived from a lower concentration of 1 M LiFSI DEE proves ineffective in preventing active substance leaching and demonstrates inferior cyclic stability. Studies indicate a direct correlation between the interfacial composition of the SPAN cathode and the electrolyte solvation structure. Promoting the ratio of anions in Li-ion solvation shells can boost the presence of anion-derived species. Based on this understanding, many ether solvents have been explored for high concentration electrolyte (HCE)/LHCE in Li-SPAN batteries, such as DME, dibutyl ether (DBE), hexyl methyl ether (HME), 1,2-diethoxyethane (1,2-DEE), etc.[50,68–70]

The electrolyte solvation structure depends on the relative ability of the solvent and anion to compete for Li ions. In highly solvating electrolytes, solvents exhibit strong competition for Li-ions, leading to a solvent-dominated solvation shell.[66] In this case, increasing electrolyte concentration is a viable method to enhance the quantity of anions in the solvation shell. Common designs of HCE and LHCE are based on this idea.[71] By introducing HCE/LHCE electrolytes, the performance of Li-SPAN cells can indeed be enhanced, but this comes at the expense of sacrificing cost and energy density. In contrast, solvents with low solvation power exhibit diminished complexation abilities and are competitively disadvantaged in coordinating with anions. This allows for the formation of an anion-rich solvation structure in the corresponding electrolyte at low concentrations (<2 M).[51,69,72,73] Ma et al. designed a low concentration, cost-effective ether electrolyte for Li-SPAN full cells, utilizing weakly solvating butyl methyl ether (BME) as the sole solvent.[48] Due to BME equipping only one ether oxygen bond, it demonstrates weaker complexation capabilities, placing it at a competitive disadvantage against anions in the Li-ion competition process. Consequently, compared to conventional electrolytes employing DME solvent with dual ether oxygen bond, anions in the

BME electrolyte predominantly exist in the contact ion pair (CIP) and aggregated structure (AGG) forms. During discharge, the anion-rich solvation structure enables the building of a robust CEI layer on the SPAN surface, effectively impeding the leaching of polysulfides, leading to reversible solid-solid conversion (Figure 2d). The relevant test indicates that Li-SPAN batteries utilizing a 2 M LiFSI BME electrolyte exhibit minimal dissolution polysulfide and negligible self-discharge behavior. As a result, Li-SPAN pouch cells under lean electrolyte and 5% excess Li conditions can stably cycle more than 40 cycles (Figure 2e).[48] Similarly, other ether-based weakly solvating electrolyte (WSE) for Li-SPAN batteries have been reported, such as DBE, DEE, dimethoxymethane, etc.[51,74,75] It's worth noting that these ether-based WSE usually demonstrate excellent low-temperature performance. For instance, when Li-SPAN batteries are equipped with 1 M LiFSI DEE electrolyte, it still works normally even at −60 °C (Figure 2f).[51]

2.3. Other Liquid Electrolyte

In addition to conventional ethers and esters, alternative solvents have been explored for application in Li-SPAN cells, such as ionic liquid, phosphate, heterocycle, etc.[76–79] Of particular interest are siloxanes, known for their low toxicity and environmental compatibility. Silicon (Si), with its 3 d empty orbital, can accept lone pair electrons from adjacent atoms, forming d-p conjugation and resulting in a stronger chemical bond.[82] Notably, the presence of d-p conjugation reduces the electron cloud density of oxygen, leading to a lower polarity in the molecule. This characteristic not only exhibits reduced solubility for polysulfides but also contributes to the formation of an anion-dominated solvation structure in the corresponding electrolyte.[49,80,82] Li et al. were pioneers in introducing siloxanes into Li-SPAN batteries, with dimethyldimethoxysilane (DMMS) as a solvent, proposing a 1.5 M LiFSI DMMS electrolyte formulation.[49] Density functional theory (DFT) calculations reveal that, compared to DME, DMMS demonstrates a lower affinity for polysulfides. Experimental dissolution studies confirm this, as Li_2S_6 exhibits extremely low solubility in DMMS solvent (Figure 3a). Furthermore, the DMMS electrolyte features an anion-rich solvation structure, facilitating the formation of a firm CEI layer for SPAN, effectively inhibiting the dissolution of polysulfides (Figure 3b). As a result, Li-SPAN cells demonstrate outstanding lifespan, the capacity retention rate was 96.9% for 300 cycles.

Similarly, Lu et al. introduced a fluorinated siloxane (FPDMS) as a solvent and formulated a 2 M LiFSI FPDMS electrolyte for Li-SPAN batteries.[80] Analysis of the molecular electrostatic potential revealed that, in comparison to commonly used ester solvents (EC, FEC, and DMC), oxygen in FPDMS exhibits a more positive charge (Figure 3c), suggesting lower solvation energy. This endows the corresponding FPDMS electrolyte with an anion-rich solvation structure. Further analysis of the composition of CEI on SPAN revealed that CEI film derived from FPDMS electrolyte is thinner and contains a higher proportion of inorganic components (LiF, LiN_xO_y, and Li_2S_x) than regular ester electrolyte (1 M $LiPF_6$ EC DMC + 10% FEC), contributing to faster

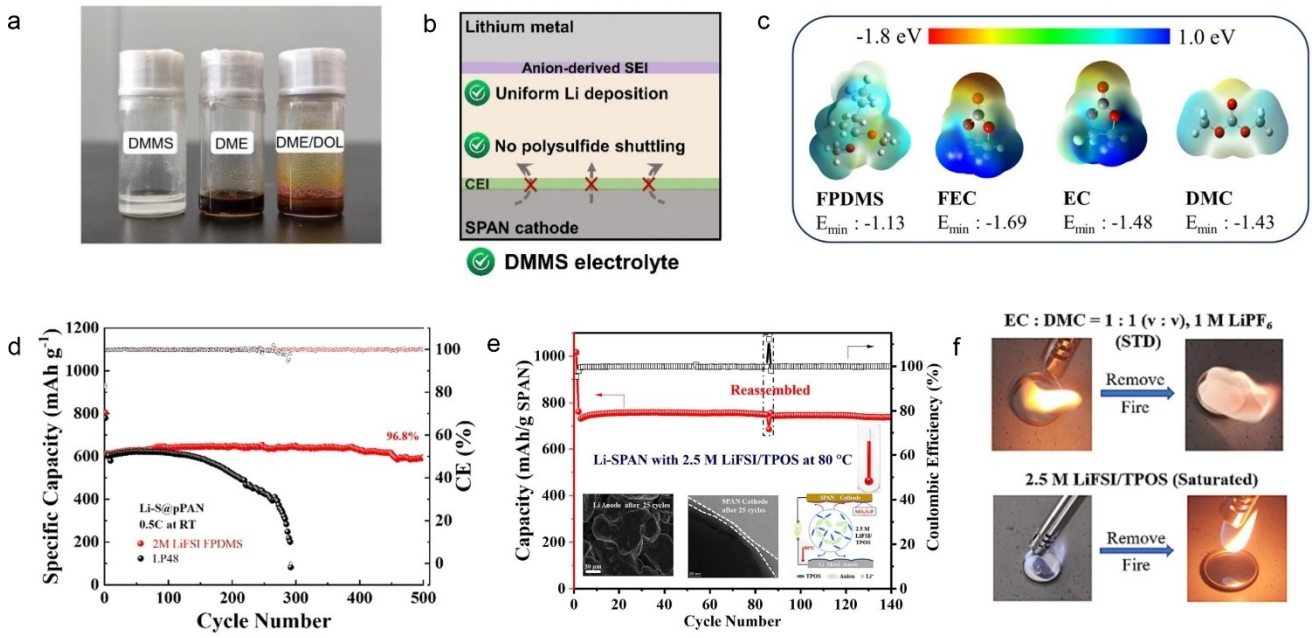

Figure 3. a) Solubility test of polysulfides in different solvents. b) Schematic illustration of the influence of DMMS electrolyte for Li-SPAN battery. Reproduced from ref. [49] Copyright (2023), with permission from Royal Society of Chemistry. c) Electrostatic potential maps of FPDMS, FEC, EC, and DMC solvent. d) Long-term cycle performance of Li-SPAN cells in different electrolytes. Reproduced from ref. [80] Copyright (2023), with permission from Elsevier. e) Long-term cycle performance of Li-SPAN cell in 2.5 M LiFSI TPOS electrolyte at 80 °C, the Insets from left to right are the Li anode morphology after 25 cycles with 2.5 M LiFSI TPOS, the SPAN morphology after 25 cycles with 2.5 M LiFSI TPOS, and the schematic diagram of the influence of 2.5 M LiFSI TPOS electrolyte for Li-SPAN battery. f) Combustion experiments of different electrolytes. Reproduced from ref. [81] Copyright (2024), with permission from Elsevier.

Li ions transport kinetics. As a result, compared to regular ester electrolyte, Li-SPAN cell employs 2 M LiFSI FPDMS electrolyte provided better electrochemistry performance, with a capacity retention rate of 96.8% after 500 cycles (Figure 3d).

Flammability is a major drawback of liquid electrolytes, posing significant challenges for the practical application of Li-SPAN batteries. In the event of a short circuit, the resulting thermal runaway within the battery can lead to combustion, highlighting the critical need for designing flame-retardant electrolytes. In response, Ma et al. developed inherently non-flammable electrolytes using tetrapropoxysilane (TPOS) as a solvent, and proposed a 2.5 M LiFSI TPOS electrolyte formulation.[81] The TPOS electrolyte equips the unique anion-rich solvation chemistry of the siloxane series electrolyte, which can form a LiF-rich electrode interface and support the stable operation of Li-SPAN cells at 80 °C (Figures 3e, f). Yang et al. developed a highly secure electrolyte formulation for Li-SPAN batteries, incorporating common flame retardant triethyl phosphate (TEP) and the high-flashpoint solvent 1,1,2,2-tetrafluoroethyl-2,2,3,3-tetrafluoropropyl ether (TTE).[77] This formulation underwent rigorous ignition testing, conclusively demonstrating its inherent flame-retardant properties. The exceptional thermal stability of this TEP/TTE based electrolyte ensures Li-SPAN batteries work stably at 60 °C.

3. Impact of Electrolyte on the Li Metal Anode

As an integral component, the compatibility between the electrolyte and the Li anode side is a crucial consideration. Given that Li-SPAN batteries directly utilize metallic Li as the anode, they inevitably face a series of challenges stemming from the Li metal.[40–42] During the plating/stripping process, the inherent chemical reactivity and high volume changes of Li metal result in low CE, thereby limiting the cycling lifespan of Li-SPAN batteries.[85] Furthermore, the Li plating process may lead to the formation of dendritic structures, which exposes Li metal batteries (LMBs) to potential short-circuit and thermal runaway threats.[38] Under low the ratio of negative to positive capacity (N/P) and lean electrolyte conditions, the issue of Li anode becomes increasingly prominent, posing a major challenge that significantly limits the cycle life of Li-SPAN batteries. Table 1 comprehensively compiles recent endeavors focused on elevating the electrochemical performance of Li-SPAN batteries under practical operating conditions through electrolyte optimization strategies. As evident from the table, the electrochemical performance of Li-SPAN batteries under low N/P ratio and lean electrolyte conditions is far less impressive. The electrolyte not only serves as an ion transport medium but also plays a significant role in interfacial chemistry. By influencing desolvation, interfacial film composition and kinetic parameters, the electrolyte impacts Li deposition behavior. Therefore, the electrolyte composition is closely linked to the cycling lifespan and safety of Li-SPAN batteries. Subsequently, we will delve into the influence of electrolytes on Li anode and Li deposition behavior.

3.1. SEI Layer

The extremely low standard electrode potential (−3.04 V vs. standard hydrogen electrode) of Li metal imparts it with high chemical reactivity, which accounts for its thermodynamic instability towards almost all solvents. When Li metal contact with the electrolyte, a heterogeneous SEI film with a "mosaic" structure is spontaneously generated.[33,34] In typical highly solvating electrolytes, the solvation structure, which is dominated by solvent molecules, tends to form an organics-dominated SEI film on the Li metal surface. These organic substances typically reveal low mechanical strength and struggle to withstand the volume changes during the Li plating/stripping process.[37] Additionally, organics present a more pronounced swelling effect in the electrolyte, causing instability in the SEI film structure.[86] In contrast, inorganics possess greater physical and chemical stability. Additionally, inorganics have a higher ionic transport capability, which effectively alleviates Li dendrites growth.[87,88] Particularly at low temperatures, inorganics exhibit lower ionic transport activation energy, rendering their conductivity relatively insensitive to temperature variations and promoting more uniform Li deposition.[89] Furthermore, inorganics offer superior electrochemical stability, which effectively prevents quantum tunneling and inhibits continuous growth of the SEI layer.[90]

$LiNO_3$ possesses strong oxidizing properties, allowing it to spontaneously react with Li metal and form an SEI film composed of Li_3N, Li_2O, and LiN_xO_y.[91] This formation effectively reduces the ionic transport barrier within the SEI, improving Li deposition behavior.[92] However, the inherent insolubility of $LiNO_3$ presents a challenge, necessitating the use of high-polarity solvents to facilitate significant dissolution. In addition, certain solubilizing agents, such as boron trifluoride, tris(pentafluorophenyl)borane, dimethyl sulfoxide, tin trifluoromethanesulfonate, γ-butyrolactone are utilized to break the solubility limit of $LiNO_3$.[93–97] FEC is a common electrolyte additive that is frequently employed to enhance the composition of the SEI layer. FEC possesses a lower lowest unoccupied molecular orbital energy level compared to most solvents and Li salts, making it highly prone to preferential solvent reduction and formation of a LiF-rich SEI.[98,99] Numerous reports indicate that the LiF-rich SEI layer exhibits lower interfacial impedance, effectively suppressing Li dendrite growth and enhancing the cycling stability of Li anodes.[101]

To enhance ionic conductivity, conventional electrolytes often employ high polarity solvents, which facilitate the disruption of electrostatic interactions between cations and anions, with the solvation structure primarily driven by solvent molecules. During the reductive decomposition process in the electrolyte, the Li metal surface generates a solvent-derived SEI layer, typically organic compounds that lack the mechanical strength required to resist Li dendrite penetration (Figure 4a).[83] In contrast, the SEI derived from an anion-rich solvation structure mainly consists of anionic derivatives. Research corroborates that the main products derived from anions are predominantly inorganic, such as LiF and Li_2O, which display superior physical, chemical, and electrochemical

Table 1. Summary of electrochemical performances of Li-SPAN batteries using different electrolytes under actual working conditions.

Electrolyte	Temperature	Battery type	Loading	N/P	E/C	Current density	Cycle life	Ref.
1.8 M LiFSI DEE/BTFE	N/A	Coin cell	>3.5 mAh cm^{-2}	~0.95	~9.5 μL mAh^{-1}	1.75 mA cm^{-2}	300 cycles, >25%	[57]
2 M LiFSI BME	25 °C	Pouch cell	~4.3 mAh cm^{-2}	1.05	3 g Ah^{-1}	0.1 C	47 cycles, 88.7%	[48]
1.8 M LiFSI DME/BTFE	25 °C	Pouch cell	~8 mAh cm^{-2}	2.5	3 g Ah^{-1}	0.2 A	>70 cycles, ~100%	[70]
2 M LiFSI FPDMS	Room temperature	Coin cell	4 mAh cm^{-2}	1.3	$m_{electrolyte}/m_{SPAN}=2.5$	0.1 C	>70 cycles, >90%	[80]
MOF-4 M LiTFSI DME	60 °C	Pouch cell	8.4 mAh cm^{-2}	2.38	1.33 g Ah^{-1}	0.15 C	100 cycles, 69.7%	[110]
2 M LiFSI DBE	23 °C	Pouch cell	~3.3 mAh cm^{-2}	2	~7 μL/mg$_{SPAN}$	0.05 A g^{-1}	50 cycles, >85%	[74]
	50 °C						30 cycles, >70%	
$[LiFSI]_1[EmimFSI]_2[Anisole]_6$	N/A	Coin cell	2.8 mg$_{SPAN}$ cm^{-2}	2.5	20 μL/cell	0.33 C charge, 1 C discharge	350 cycles, 90%	[111]
LiFSI:DME:OFE	N/A	Pouch cell	7.5 mAh cm^{-2}	2	2.4 g Ah^{-1}	0.1 C	70 cycles, ~100%	[112]
$[LiFSI]_1[EmimFSI]_2[mFBn]_2$	N/A	Coin cell	2.7 mg$_{SPAN}$ cm^{-2}	1.8	~10.6 mL Ah^{-1}	0.33 C charge, 1 C discharge	250 cycles, 71%	[76]
1.7 M LiFSI TEP/DBE	30 °C	Pouch cell	3.5 mAh cm^{-2}	2.4	3 g Ah^{-1}	0.2 C	65 cycles, >70%	[113]
1 M LiFSI MTFP/FEC	50 °C	Coin cell	~3.5 mAh cm^{-2}	~1.7	2 g Ah^{-1}	0.05 A g^{-1}	80 cycles, >50%	[114]
	23 °C					0.1 A g^{-1}	180 cycles, >60%	
	−40 °C					0.05 A g^{-1}	50 cycles, >40%	
1 M LiFSI DEE	23 °C	Coin cell	3.5 mAh cm^{-2}	1	75 μL/cell	0.33 C	50 cycles, >60%	[51]
	−40 °C					0.2 C	50 cycles, >50%	
	−60 °C					0.2 C	50 cycles, >30%	

characteristics.[102,103] It helps to improve the interface stability of the Li metal and increase the plating/stripping reversibility. Additionally, as the quantity of anions in the solvation structure escalates, there is a corresponding synchronous increase in the content of anion derivatives within the interfacial chemistry.[104] Consequently, a considerable portion of research in electrolyte design pivots around increasing the number of anions in the solvent sheath.

To construct an anion-rich solvation structure, it is typically achieved through the design of HCE, LHCE, and WSE (Figure 4b).[71] In the case of HCE, this is accomplished by increasing the amount of Li salts to squeeze out solvent molecules from the solvation sheath. While the introduction of HCE can notably improve the quality of the SEI layer, it also suffers from high cost, elevated viscosity, and poor wettability.[105] To address this, researchers have introduced low viscosity hydrofluoroether (HFE) as a diluent to overcome these shortcomings. HFE typically features fluoroalkyl groups at the α or β position. Under the strong electron-withdrawing effect of fluorine (F), the electron cloud density of oxygen in HFE diminishes, resulting in a marked decrease in its coordination capability. As an "inert" constituent, HFE does not partake in the solvation structure.[66,106] Consequently, LHCE can maintain a solvation structure akin to that of the corresponding HCE. Although the use of HFE can avoid the disadvantages of HCE, its high price makes it difficult to achieve large-scale commercialization.[107] Subsequently, researchers focused on developing low-cost diluents. Suo proposed an LHCE utilizing the more economical hexane (HEX) as a diluent.[69] HEX not only suppresses solvent reduction but also weakens the interaction between Li ions and solvents, facilitating Li ions desolvation, leading to a high CE for Li anode (99.59% at 25 °C, 99.30% at 60 °C and 98.75% at −30 °C). Dong et al. employed low-viscosity and cost-effective dichloromethane as a diluent for their LHCE formulation, achieving the operation of LMBs at −70 °C.[108] Yoo et al. developed an LHCE using inexpensive 1,2-difluorobenzene as the diluent, which not only possesses the characteristics of a conventional HFE, but also exhibits a high chemical reactivity to

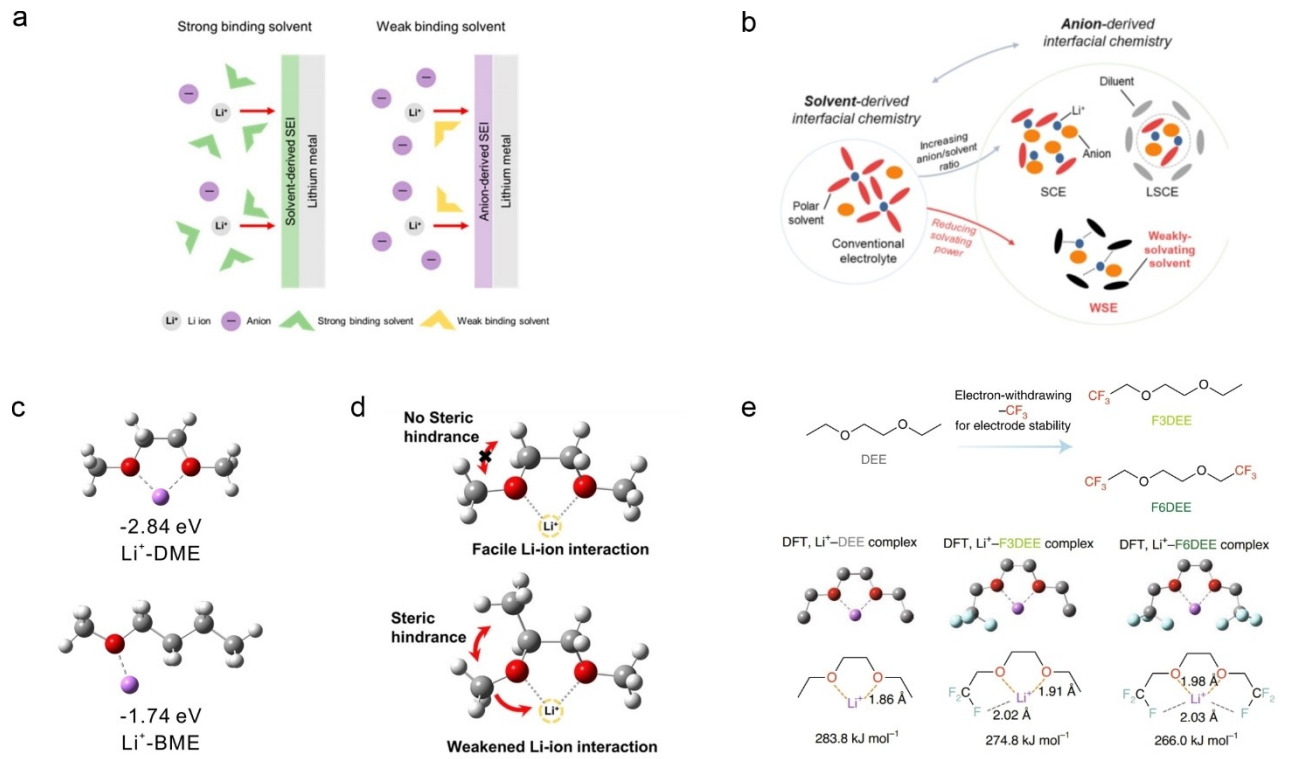

Figure 4. a) The relationship between coordination capacity of solvents and interfacial chemistry. Reproduced from ref. [83] Copyright (2021), with permission from American Chemical Society. b) The relationship between solvent solvating power and solvation structure. Reproduced from ref. [71] Copyright (2021), with permission from Wiley-VCH. c) Optimized structures and binding energy of Li-ion complexes with DME and BME. Reproduced from ref. [48] Copyright (2023), with permission from Wiley-VCH. d) Schematic illustration of steric hindrance and interaction with Li-ion for DME and DMP. Reproduced from ref. [72] Copyright (2023), with permission from American Chemical Society. e) Relationship between F content and complexation capacity in DEE solvent. Reproduced from ref. [84] Copyright (2022), with permission from Springer Nature.

Li metal. It allows 1,2-difluorobenzene to participate in the formation of the SEI layer and facilitate an enhancement in LiF content.[105]

To enhance interaction between cation and anion, in addition to increasing electrolyte concentration, the use of low solvation power solvents represents another effective approach (Figure 4b). Low solvation power solvents exhibit poor complexation ability with Li ions, placing them at a disadvantage in competing with anions for the Li ions solvation shell. This allows for the construction of an anion-rich solvation structure at low concentrations (1–2 M). WSE not only possesses the unique anion-rich solvation chemistry like HCE/LHCE, but also alleviates issues such as high viscosity, high cost, and low wettability.[71,109] In 2021, Yao et al. introduced the concept of WSE and utilized low-polarity solvents to construct low-concentration electrolytes (1 M) with abundant CIP and AGG structures.[71] The core concept of designing WSE is to minimize the interaction between Li ions and solvents. From the perspective of solvent selection, solvents possessing low solvating power are preferred. The solvating power of solvent can be assessed based on DFT calculations of the binding energy between Li ions and solvents, where a more positive value indicates lower complexation capabilities. In experimental terms, Kim et al. proposed a potential measurement technique to assess the relative solvation of Li ions in electrolytes.[83] To this end, the authors assembled an H-type electrochemical cell and introduced the test and reference electrolytes into two half-cells, connected by a salt bridge. By measuring the open-circuit voltage of the electrochemical cell, the solvation energy of the test electrolyte can be evaluated. A greater negative potential indicates higher solvation free energy, indicative of weaker binding between Li ions and the solvent. Additionally, the authors utilized cryo-electron microscopy to observe that weaker solvation facilitates the formation of a SEI layer that is dominant by anion-derived species. This further confirms the intrinsic relationship between solvation structure and interfacial chemistry.

For designing WSE, it is preferable to use solvents with fewer functional groups. For instance, DME, a commonly used ether solvent, contains two ether oxygen bonds, enabling the formation of a stable six-membered ring coordination structure with Li ions. In contrast, solvents such as DEE, DBE, HME, and BME only contain a single ether oxygen bond, resulting in significantly weaker interaction (Figure 4c). Consequently, more CIP and AGG structures can be found in electrolytes with fewer functional group solvents. Another approach involves increasing steric hindrance (Figure 4d). 1,2-DEE, a solvent akin to DME, possesses dual ether oxygen functional groups. The key distinction lies in the terminal groups: 1,2-DEE terminates with an ethyl group, whereas DME terminates with a methyl group. As a result, 1,2-DEE with the ethyl group can induce a stronger steric hindrance effect, leading to lower solvent molecules in the solvation structure of the electrolyte.[73] Similarly, Park et al.

proposed the use of 1,2-dimethoxypropane (DMP) as a solvent for electrolytes.[72] The steric hindrance effect in DMP forces the methoxy carbon in DMP to be far away from the ethyl main chain, reducing overall charge separation and effectively weakening the solvation capability of solvent molecules, inducing the formation of a large number of CIP and AGG structures in the electrolyte, as well as induced the formation of an anion-driven SEI layer.

Another method is to reduce the charge density on the functional groups of solvents (Figure 4e). F possesses the lowest electronegativity (3.9) among all elements, making it a suitable component for reducing electron cloud density. Introducing F or trifluoromethyl to solvent can diminish their complexation ability. Based on this concept, numerous new fluorinated solvent molecules have been reported. Unlike HFE, fluorinated solvents exhibit strong interactions with Li ions and dissolve a certain amount of Li salts. Due to the decrease of the charge density of the functional groups, the ability of the solvent molecules to complex Li ions decreases sharply, which tends to increase the cation – anion interaction in corresponding electrolytes. Cui's and other groups designed and synthesized a large number of new fluorinated solvent molecules, which have been employed as electrolyte solvents to improve the interfacial chemistry of Li metal as well as Li plating/stripping reversibility.[84,115–118] Even so, the high cost of raw materials for the synthesis of novel fluorinated solvents is expected to markedly escalate the manufacturing cost of cells.

3.2. Desolvation Process

The solvent structure of the electrolyte not only influences the composition/structure of the SEI layer, but also determines the Li-ion desolvation process.[48,51,75,119] The desolvation process is closely related to the Li plating behavior, and rapid desolvation can achieve uniform deposition morphology, thereby inhibiting Li dendrite growth.[51,120] Relevant studies have shown that, during the Li ions desolvation process, Li metal surface with negative charge repels to anions, so the electrostatic interaction between anions and Li ions can be ignored.[121–124] Therefore, the difficulty of the entire desolvation process depends on the number of solvent molecules and the solvation capacity in the Li ions solvent shell. For conventional electrolytes (using high solvating power solvents), the solvation structure is dominated by the association between Li ions and solvent molecules, resulting in a higher Li-ion desolvation barrier, and the corresponding electrolyte suffers from severe dendrite Li growth.[75] For electrolytes with fewer solvent molecules in the solvation structure, such as HCE, LHCE, and WSE, there reveal a low desolvation barrier and tends to exhibit uniform Li deposition morphology and high CE of Li metal anode.[51,69,119,125] Recent research has discovered that, despite diluents not being directly participate in solvation, they exhibit dipole-dipole interactions with solvent molecules.[69,126–128] It weakens the interplay between Li ions and solvents, while concurrently intensifying the interaction between Li ions and anions, leading to a faster Li ions desolvation process.

3.3. Mass Transport Property

The desirable concentration for commercial electrolytes is approximately 1 M, as this proportion yields the highest ionic conductivity.[67,129] Enhancing ion conductivity is considered a primary factor in the electrolyte design for LIBs. However, for LMBs, the Li deposition behavior is not necessarily correlated with the magnitude of ion conductivity. In fact, in certain low ion conductivity electrolytes, remarkably high Li deposition/stripping efficiency (>99%) can be observed.[48,51,75] Li ions transference number is utilized to evaluate the contribution of cations to the total conductivity in the electrolyte. In dilute electrolytes, Li ions transfer primarily via a vehicular mechanism, where Li ions move with their solvation shell (Figure 5a).[130] Due to the confinement by solvent molecules, the migration rate of

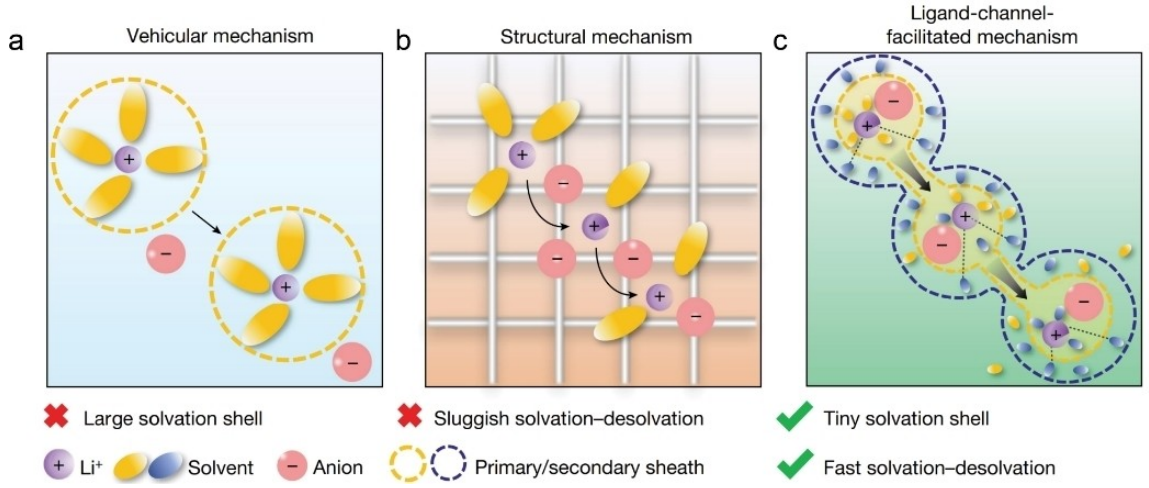

Figure 5. Transport mechanism of Li ions in different electrolytes: a) dilute electrolytes, b) HCE, c) WSE with small solvent molecules. Reproduced from ref. [100] Copyright (2024), with permission from Springer Nature.

Li ions is lower than that of anions, resulting in Li ions transference number below 0.5.[131,132] Within LMBs, anions tend to migrate in the opposite direction to Li ions and accumulate on the electrode surface,[130] leading to the accumulation of concentration gradients and triggering Li dendrite growth.[133] Particularly at high rates, the concentration polarization stemming from low Li ions transference number becomes more pronounced. In HCE, the structure mechanism dominates Li ions transfer, in which Li ions hop between adjacent solvation sites (Figure 5b).[131] For LHCE, the ion transport mode is similar to HCE, except that the diluent interrupts the continuous ion hop.[131,134] Under the action of this special ion transport mechanism, a high Li ions transference number can be observed in the HCE/LHCE.[128,131,135] For WSE with low small solvent molecules, Li ions execute the channel-facilitated mechanism (Figure 5c).[100] In this process, solvents in the secondary solvation sheath enable interaction with Li ions in the primary solvation sheath from the Li ions transport channels, leading to remarkable ion transport kinetics and transference number.

4. Summary and Outlook

Li-SPAN batteries, leveraging multi-electron transfer reactions, exhibit remarkable energy density, albeit with a shorter cycle life compared to conventional Li-ion batteries. This characteristic positions them ideally for applications that prioritize high energy density over exceptional cycling longevity. Consequently, Li-SPAN batteries are highly likely to be employed in unmanned aerial vehicles or electric aircraft that demand prolonged, heavy-load flights. In these applications, the ability to carry more energy in a smaller and lighter package is crucial for maximizing flight time and range. However, this system faces challenges with electrolyte compatibility. Conventional electrolytes fail to address both the dissolution of polysulfides in the SPAN cathode and Li dendrite growth at the Li metal anode simultaneously, resulting in limited battery cycle life. For the SPAN cathode, its conversion mechanism varies in different types of electrolytes. In conventional ester-based electrolytes (containing cyclic ester solvents, such as EC and FEC), SPAN undergoes solid-solid conversion, exhibiting excellent cycling stability. Further investigations reveal the crucial role of cyclic ester electrolytes in stabilizing the SPAN cathode, as they facilitate the formation of a stable interfacial film that prevents the leaching of polysulfides from the SPAN material. However, conventional ester-based electrolytes suffer from Li dendrites. In contrast, a better Li plating behavior can be found in conventional ether-based electrolytes. While the stability of the derived CEI film from solvent molecules is poorer, failing to inhibit the dissolution of intermediate products during the charge/discharge processes of the SPAN cathode, resulting in inferior battery cycling performance. Additionally, certain common film-forming compounds can effectively enhance the interfacial stability of SPAN, such as $LiNO_3$, LiBOB, and LiODFB. Essentially, the type of electrolyte is not the primary factor affecting the stability of the SPAN electrode, but rather the CEI layer.

Anions, as essential components of electrolytes, also exhibit good film-forming properties. Interfacial films derived from anion are rich in inorganic compounds, offering higher stability and lower impedance compared to organic-dominated interfacial films. Furthermore, with an increase in the anion content in the solvation structure, the content of inorganic compounds in the electrode interfacial film also rises concurrently. Therefore, a plethora of electrolytes with anion-rich solvation structure have been reported, including HCE, LHCE, and WSE. In these electrolytes, the interfacial film of the SPAN cathode is predominantly derived from anions, which effectively block the leaching of polysulfides and enable reversible solid-solid conversions. Additionally, such electrolytes with anion-rich solvation structures can decompose on the Li metal surface to form an excellent SEI layer, and exhibit faster desolvation kinetics and and high transference number, achieving a reversible Li deposition/stripping process. In general, the construction of anion-rich solvated structures represents the most ideal approach to enhancing the performance of Li-SPAN batteries. When applying Li-SPAN batteries to practical scenarios, in addition to focusing on their key electrochemical performance indicators like energy density and cycle life, the cost is also a significant factor that cannot be overlooked. Overall, LHCE (use low cost diluent) and WSE with low cost, low density, and high wettability, emerge as the top choice.

Despite the extensive reporting on related electrolytes, there are still several issues that urgently need to be addressed. The electrode-electrolyte interface is the main site of the electrochemical reaction, involving ions desolvation, compound decomposition, charge transfer, mass diffusion, dynamic change of double electric layer, etc. Although plenty of research on the electrolyte solvation environment has been reported, the understanding of interfacial chemistry is still lacking. Li-SPAN batteries inevitably encounter variations in operating temperatures. However, at high temperature, they are susceptible to issues such as self-discharge, gas generation, and thermal runaway. Conversely, at low temperature, they suffer from capacity degradation and a significant risk of short circuits. As a consequence, to cope with wide temperature conditions, the design of the electrolyte should take into account high/low temperature performance.

On the other hand, the safety aspect of batteries cannot be overlooked, as traditional liquid electrolytes, comprising organic small molecules, grapple with issues like flammability, volatility, poor thermal stability, narrow operating temperatures, and leakage, posing safety risks to Li-SPAN batteries. Solid state electrolytes, as the ultimate goal in battery development, alleviate these challenges with their unique solid state structure, offering superior safety. Nonetheless, solid state electrolytes encounter significant interfacial contact issues. Ion transport in solid state electrolytes follows a fundamentally different mechanism from that in liquid electrolytes, relying on intimate contacts between solid particles for rapid migration. Consequently, constructing a dense, highly compressed structure is essential. However, achieving close contact among solid

particles is hindered by disparities in surface energy, hardness, brittleness, as well as volume expansion of electrode material during the lithiation/delithiation process. For Li metal anodes, while solid state electrolytes theoretically can restrain the growth of Li dendrites, they still fall short in fully preventing their penetration. The interfacial side reaction between Li metal and solid electrolyte is another obstacle, which will lead to the continuous increase of battery polarization and rapid capacity degradation. Moreover, elevated costs and inferior ionic conductivity remain critical barriers to the widespread adoption of solid state electrolytes. In summary, integrating solid state electrolytes into Li-SPAN batteries represents an exceptional approach to achieving intrinsic safety within this chemical system. Nevertheless, numerous scientific challenges must still be overcome to fully realize this potential.

Acknowledgements

This study was supported by the National Natural Science Foundation of China (22279063), the Fundamental Research Funds for the Central Universities, and Tianjin Natural Science Foundation (No. 22JCYBJC00590). We thank the Haihe Laboratory of Sustainable Chemical Transformations for financial support.

Conflict of Interests

The authors declare no conflict of interest.

Keywords: Sulfurized polyacrylonitrile · Lithium dendrites · Cathode electrolyte interphase · Solvation structure · Solid–solid conversion

[1] J. B. Goodenough, Y. Kim, *Chem. Mater.* **2010**, *22*, 587–603.
[2] X. Shen, H. Liu, X. B. Cheng, C. Yan, J. Q. Huang, *Energy Storage Mater.* **2018**, *12*, 161–175.
[3] J. J. Xu, X. Y. Cai, S. M. Cai, Y. X. Shao, C. Hu, S. R. Lu, S. J. Ding, *Energy Environ. Mater.* **2023**, *6*, e12450.
[4] Z. Yang, H. Huang, F. Lin, *Adv. Energy Mater.* **2022**, *12*, 2200383.
[5] J. M. Du, W. Y. Wang, M. T. Wan, X. C. Wang, G. C. Li, Y. C. Tan, C. H. Li, S. B. Tu, Y. M. Sun, *Adv. Energy Mater.* **2021**, *11*, 2102259.
[6] M. Zhao, B. Q. Li, H. J. Peng, H. Yuan, J. Y. Wei, J. Q. Huang, *Angew. Chem. Int. Ed.* **2020**, *59*, 12636–12652.
[7] R. Van Noorden, *Nature* **2013**, *498*, 416–417.
[8] H. Wang, P. Zheng, H. Yi, Y. Wang, Z. Yang, Z. Lei, Y. Chen, Y. Deng, C. Wang, Y. Yang, *Macromolecules* **2020**, *53*, 8539–8547.
[9] Z. H. He, X. Y. Dou, W. L. Liu, L. X. Zhang, L. X. Lv, J. H. Liu, F. C. Meng, *Batteries* **2023**, *9*, 289.
[10] J. Liu, Y. H. Zhou, T. Y. Yan, X. P. Gao, *Adv. Funct. Mater.* **2024**, *23*, 2309625.
[11] D. W. Wang, Q. C. Zeng, G. M. Zhou, L. C. Yin, F. Li, H. M. Cheng, I. R. Gentle, G. Q. M. Lu, *J. Mater. Chem. A* **2013**, *1*, 9382–9394.
[12] A. Hu, M. Zhou, T. Lei, Y. Hu, X. Du, C. Gong, C. Shu, J. Long, J. Zhu, W. Chen, *Adv. Energy Mater.* **2020**, *10*, 2002180.
[13] P. Wang, X. Dai, P. Xu, S. Hu, X. Xiong, K. Zou, S. Guo, J. Sun, C. Zhang, Y. Liu, T. Zhou, Y. Chen, *eScience* **2023**, *3*, 100088.
[14] J. F. Li, Z. H. Niu, C. Guo, M. Li, W. Z. Bao, *J. Energy Chem.* **2021**, *54*, 434–451.
[15] Y. Z. Huang, L. Lin, C. K. Zhang, L. Liu, Y. K. Li, Z. S. Qiao, J. Lin, Q. L. Wei, L. S. Wang, Q. S. Xie, D. L. Peng, *Adv. Sci.* **2022**, *9*, 2106004.
[16] M. Zhao, X.-Y. Li, X. Chen, B.-Q. Li, S. Kaskel, Q. Zhang, J.-Q. Huang, *eScience* **2021**, *1*, 44–52.
[17] J. T. Kim, X. G. Hao, C. H. Wang, X. L. Sun, *Matter* **2023**, *6*, 316–343.
[18] Q. S. Miao, N. Solan, G. Hyun, J. Holoubek, P. Liu, *ACS Energy Lett.* **2023**, *8*, 4818–4830.
[19] B. He, Z. X. Rao, Z. X. Cheng, D. D. Liu, D. Q. He, J. Chen, Z. Y. Miao, L. X. Yuan, Z. Li, Y. H. Huang, *Adv. Energy Mater.* **2021**, *11*, 2003690.
[20] Z. Han, S. Li, R. Xiong, Z. Jiang, M. Sun, W. Hu, L. Peng, R. He, H. Zhou, C. Yu, S. Cheng, J. Xie, *Adv. Funct. Mater.* **2022**, *32*, 2108669.
[21] H. Zhang, Z. Zeng, F. Ma, Q. Wu, X. Wang, S. Cheng, J. Xie, *Angew. Chem. Int. Ed.* **2023**, *135*, e202300771.
[22] S. Wang, B. Y. Lu, D. Y. Cheng, Z. H. Wu, S. J. Feng, M. H. Zhang, W. K. Li, Q. S. Miao, M. Patel, J. Q. Feng, E. Hopkins, J. B. Zhou, S. Parab, B. Bhamwala, B. Liaw, Y. S. Meng, P. Liu, *J. Am. Chem. Soc.* **2023**, *145*, 9624–9633.
[23] Y. Z. Fu, A. Manthiram, *RSC Adv.* **2012**, *2*, 5927–5929.
[24] X. H. Zhao, C. L. Wang, Z. W. Li, X. C. Hu, A. A. Razzaq, Z. Deng, *J. Mater. Chem. A* **2021**, *9*, 19282–19297.
[25] X. Y. Zhang, K. Chen, Z. H. Sun, G. J. Hu, R. Xiao, H. M. Cheng, F. Li, *Energy Environ. Sci.* **2020**, *13*, 1076–1095.
[26] T. N. L. Doan, M. Ghaznavi, Y. Zhao, Y. Zhang, A. Konarov, M. Sadhu, R. Tangirala, P. Chen, *J. Power Sources* **2013**, *241*, 61–69.
[27] X. Li, L. Yuan, D. Liu, J. Xiang, Z. Li, Y. Huang, *Small* **2022**, *18*, 2106970.
[28] D. C. Lin, Y. Y. Liu, Y. Cui, *Nat. Nanotechnol.* **2017**, *12*, 194–206.
[29] Z. Y. Shen, W. D. Zhang, S. L. Mao, S. Y. Li, X. Y. Wang, Y. Y. Lu, *ACS Energy Lett.* **2021**, *6*, 2673–2681.
[30] H. J. Yang, A. Naveed, Q. Y. Li, C. Guo, J. H. Chen, J. Y. Lei, J. Yang, Y. N. Nuli, J. L. Wang, *Energy Storage Mater.* **2018**, *15*, 299–307.
[31] Z. X. Xu, J. L. Wang, J. Yang, X. W. Miao, R. J. Chen, J. Qian, R. R. Miao, *Angew. Chem. Int. Ed.* **2016**, *55*, 10372–10375.
[32] F. Jin, C. Hu, C. Liu, Y. Zheng, H. Chen, Y. Shen, L. Chen, *J. Electroanal. Chem.* **2019**, *835*, 156–160.
[33] H. Wu, H. Jia, C. Wang, J. G. Zhang, W. Xu, *Adv. Energy Mater.* **2021**, *11*, 2003092.
[34] O. Sheng, H. Hu, T. Liu, Z. Ju, G. Lu, Y. Liu, J. Nai, Y. Wang, W. Zhang, X. Tao, *Adv. Funct. Mater.* **2022**, *32*, 2111026.
[35] W. Xu, J. L. Wang, F. Ding, X. L. Chen, E. Nasybutin, Y. H. Zhang, J. G. Zhang, *Energy Environ. Sci.* **2014**, *7*, 513–537.
[36] Y. Wu, C. Wang, C. Wang, Y. Zhang, J. Liu, Y. Jin, H. Wang, Q. Zhang, *Mater. Horiz.* **2024**, *11*, 388–407.
[37] R. D. Deshpande, D. M. Bernardi, *J. Electrochem. Soc.* **2017**, *164*, A461.
[38] G. X. Zhang, X. Z. Wei, X. Tang, J. G. Zhu, S. Q. Chen, H. F. Dai, *Renew. Sustain. Energy Rev.* **2021**, *141*, 110790.
[39] K. Xu, *Chem. Rev.* **2014**, *114*, 11503–11618.
[40] W. Li, P. Luo, M. H. Chen, X. P. Lin, L. Du, H. Y. Song, Y. H. Lu, Z. M. Cui, *J. Mater. Chem. A* **2022**, *10*, 15161–15168.
[41] J.-N. Chazalviel, *Phys. Rev. A* **1990**, *42*, 7355.
[42] Q. Lyu, P. F. Dai, A. G. Chen, *Composites, Part B* **2024**, *268*, 111079.
[43] F. Ding, W. Xu, X. L. Chen, J. Zhang, M. H. Engelhard, Y. H. Zhang, B. R. Johnson, J. V. Crum, T. A. Blake, X. J. Liu, J. G. Zhang, *J. Electrochem. Soc.* **2013**, *160*, A1894–A1901.
[44] S. Y. Yuan, T. Y. Kong, Y. Y. Zhang, P. Dong, Y. J. Zhang, X. L. Dong, Y. G. Wang, Y. Y. Xia, *Angew. Chem. Int. Ed.* **2021**, *60*, 25624–25638.
[45] Z. Han, S. Li, M. Sun, R. He, W. Zhong, C. Yu, S. Cheng, J. Xie, *J. Energy Chem.* **2022**, *68*, 752–761.
[46] Y. K. Yi, F. Hai, J. Y. Guo, X. L. Tian, S. T. Zheng, Z. D. Wu, T. Wang, M. T. Li, *Batteries* **2023**, *9*, 27.
[47] X. Chen, L. Peng, L. Wang, J. Yang, Z. Hao, J. Xiang, K. Yuan, Y. Huang, B. Shan, L. Yuan, J. Xie, *Nat. Commun.* **2019**, *10*, 1021.
[48] T. Ma, Y. X. Ni, D. T. Li, Z. T. Zha, S. Jin, W. J. Zhang, L. Q. Jia, Q. Sun, W. W. Xie, Z. L. Tao, J. Chen, *Angew. Chem. Int. Ed.* **2023**, *62*, e202310761.
[49] M. Li, H. Chen, Y. Wang, X. Chen, J. Wu, J. Su, M. Wang, X. Li, C. Li, L. Ma, *J. Mater. Chem. A* **2023**, *11*, 11721–11729.
[50] J. J. Zhou, Y. S. Guo, C. D. Liang, L. J. Cao, H. Pan, J. Yang, J. L. Wang, *Chem. Commun.* **2018**, *54*, 5478–5481.
[51] J. Holoubek, H. Liu, Z. Wu, Y. Yin, X. Xing, G. Cai, S. Yu, H. Zhou, T. A. Pascal, Z. Chen, *Nat. Energy* **2021**, *6*, 303–313.
[52] J. Xiang, Z. Guo, Z. Yi, Y. Zhang, L. Yuan, Z. Cheng, Y. Shen, Y. Huang, *J. Energy Chem.* **2020**, *49*, 161–165.
[53] Y. Wang, Y. P. Zhang, Y. Shuai, K. H. Chen, *Energy* **2021**, *233*, 121160.
[54] A. L. Paez Jerez, D. M. Chemes, E. L. Sham, L. E. Davies, A. Y. Tesio, V. Flexer, *ChemistrySelect* **2020**, *5*, 5465–5472.

[55] Z. H. Wu, S. M. Bak, Z. Shadike, S. C. Yu, E. Y. Hu, X. Xing, Y. H. Du, X. Q. Yang, H. D. Liu, P. Liu, *ACS Appl. Mater. Interfaces* **2021**, *13*, 31733–31740.
[56] J. Holoubek, Q. Z. Yan, H. D. Liu, Z. H. Wu, X. Xing, H. Y. Zhou, J. Luo, Z. Chen, P. Liu, *ACS Appl. Energy Mater.* **2021**, *4*, 6422–6429.
[57] H. Liu, J. Holoubek, H. Zhou, A. Chen, N. Chang, Z. Wu, S. Yu, Q. Yan, X. Xing, Y. Li, T. A. Pascal, P. Liu, *Mater. Today* **2021**, *42*, 17–28.
[58] J. Li, Z. Fan, J. Guo, J. Zheng, W. Xie, Z. Fang, C. Yan, R. Wang, H. Chen, H. He, *Surf. Interfaces* **2024**, *48*, 104309.
[59] K. P. Yu, G. R. Cai, M. Q. Li, J. L. Wu, V. Gupta, D. J. Lee, J. Holoubek, Z. Chen, *ACS Appl. Mater. Interfaces* **2023**, *15*, 43724–43731.
[60] J. Tan, M. X. Ye, J. F. Shen, *Mater. Horiz.* **2022**, *9*, 2325–2334.
[61] D. Aurbach, E. Pollak, R. Elazari, G. Salitra, C. S. Kelley, J. Affinito, *J. Electrochem. Soc.* **2009**, *156*, A694.
[62] X. Xing, Y. J. Li, X. F. Wang, V. Petrova, H. D. Liu, P. Liu, *Energy Storage Mater.* **2019**, *21*, 474–480.
[63] J. Y. Luo, Z. Y. Chen, R. Z. Zhang, C. B. Lu, J. H. Zhu, X. D. Zhuang, *Electrochim. Acta* **2024**, *474*, 143533.
[64] F. Qiu, S. Ren, X. Zhang, P. He, H. Zhou, *Sci. Bull.* **2021**, *66*, 897–903.
[65] C. Zhang, Q. Lan, Y. Liu, J. Wu, H. Shao, H. Zhan, Y. Yang, *Electrochim. Acta* **2019**, *306*, 407–419.
[66] X. Cao, H. Jia, W. Xu, J.-G. Zhang, *J. Electrochem. Soc.* **2021**, *168*, 010522.
[67] G. A. Giffin, *Nat. Commun.* **2022**, *13*, 5250.
[68] J.-M. Kim, P. Gao, Q. Miao, Q. Zhao, M. M. Rahman, P. Chen, X. Zhang, E. Hu, P. Liu, J.-G. Zhang, W. Xu, *ACS Appl. Mater. Interfaces* **2024**, *16*, 20618–20625.
[69] T. Liu, J. N. Feng, Z. Shi, H. J. Li, W. A. Zhao, M. L. Mao, X. Z. Zhu, Y. S. Hu, H. Li, X. J. Huang, L. Q. Chen, L. M. Suo, *Sci. China Chem.* **2023**, *66*, 2700–2710.
[70] Z. H. Wu, H. D. Liu, J. Holoubek, C. Anderson, L. L. Shi, H. Khemchandani, D. P. Lu, D. Y. Liu, C. J. Niu, J. Xiao, P. Liu, *ACS Energy Lett.* **2022**, *7*, 2701–2710.
[71] Y. X. Yao, X. Chen, C. Yan, X. Q. Zhang, W. L. Cai, J. Q. Huang, Q. Zhang, *Angew. Chem. Int. Ed.* **2021**, *60*, 4090–4097.
[72] E. Park, J. Park, K. Lee, Y. Zhao, T. H. Zhou, G. Park, M. G. Jeong, M. Choi, D. J. Yoo, H. G. Jung, A. Coskun, J. W. Choi, *ACS Energy Lett.* **2023**, *8*, 179–188.
[73] Y. Chen, Z. Yu, P. Rudnicki, H. Gong, Z. Huang, S. C. Kim, J.-C. Lai, X. Kong, J. Qin, Y. Cui, *J. Am. Chem. Soc.* **2021**, *143*, 18703–18713.
[74] G. Cai, J. Holoubek, M. Li, H. Gao, Y. Yin, S. Yu, H. Liu, T. A. Pascal, P. Liu, Z. Chen, *Proc. Natl. Acad. Sci. USA* **2022**, *119*, e2200392119.
[75] T. Ma, Y. X. Ni, Q. R. Wang, W. J. Zhang, S. Jin, S. B. Zheng, X. Yang, Y. P. Hou, Z. L. Tao, J. Chen, *Angew. Chem. Int. Ed.* **2022**, *61*, e202207927.
[76] X. Liu, T. Diemant, A. Mariani, X. Dong, M. E. Di Pietro, A. Mele, S. Passerini, *Adv. Mater.* **2022**, *34*, 2207155.
[77] H. J. Yang, C. Guo, J. H. Chen, A. Naveed, J. Yang, Y. Nuli, J. L. Wang, *Angew. Chem. Int. Ed.* **2019**, *58*, 791–795.
[78] S. Tan, H. Liu, Z. Wu, C. Weiland, S.-M. Bak, A. Ronne, P. Liu, M. S. Whittingham, Z. Shadike, E. Hu, *J. Electrochem. Soc.* **2022**, *169*, 030513.
[79] X. Liu, A. Mariani, H. Adenusi, S. Passerini, *Angew. Chem. Int. Ed.* **2023**, *62*, e202219318.
[80] H. Lu, Q. Wang, J. Chen, H. Zhang, J. Ding, Y. Nuli, J. Yang, J. Wang, *Energy Storage Mater.* **2023**, *63*, 102994.
[81] H. Y. Ma, Q. H. Wang, H. C. Lu, Y. B. Si, X. R. Kong, J. L. Wang, *Chem. Eng. J.* **2024**, *479*, 147557.
[82] Y. Huang, R. Li, S. Weng, H. Zhang, C. Zhu, D. Lu, C. Sun, X. Huang, T. Deng, L. Fan, *Energy Environ. Sci.* **2022**, *15*, 4349–4361.
[83] S. C. Kim, X. Kong, R. A. Vilá, W. Huang, Y. L. Chen, D. T. Boyle, Z. A. Yu, H. S. Wang, Z. N. Bao, J. Qin, Y. Cui, *J. Am. Chem. Soc.* **2021**, *143*, 10301–10308.
[84] Z. Yu, P. E. Rudnicki, Z. Zhang, Z. Huang, H. Celik, S. T. Oyakhire, Y. Chen, X. Kong, S. C. Kim, X. Xiao, *Nat. Energy* **2022**, *7*, 94–106.
[85] J. M. Zhang, Q. P. Li, Y. P. Zeng, Z. Tang, D. Sun, D. Huang, Z. G. Peng, Y. G. Tang, H. Y. Wang, *Chem. Eng. J.* **2021**, *426*, 131110.
[86] Z. W. Zhang, Y. Z. Li, R. Xu, W. J. Zhou, Y. B. Li, S. T. Oyakhire, Y. C. Wu, J. W. Xu, H. S. Wang, Z. A. Yu, D. T. Boyle, W. Huang, Y. S. Ye, H. Chen, J. Y. Wan, Z. N. Bao, W. Chiu, Y. Cui, *Science* **2022**, *375*, 66–70.
[87] H.-H. Sun, A. Dolocan, J. A. Weeks, R. Rodriguez, A. Heller, C. B. Mullins, *J. Mater. Chem. A* **2019**, *7*, 17782–17789.
[88] Z. Sun, J. Yang, H. Xu, C. Jiang, Y. Niu, X. Lian, Y. Liu, R. Su, D. Liu, Y. Long, *Nano-Micro Lett.* **2024**, *16*, 141.
[89] Y. Wang, Z. Li, W. Xie, Q. Zhang, Z. Hao, C. Zheng, J. Hou, Y. Lu, Z. Yan, Q. Zhao, *Angew. Chem. Int. Ed.* **2024**, *136*, e202310905.
[90] Z. Shen, W. Zhang, S. Li, S. Mao, X. Wang, F. Chen, Y. Lu, *Nano Lett.* **2020**, *20*, 6606–6613.
[91] L. Song, D. Ning, Y. Chai, M. Ma, G. Zhang, A. Wang, H. Su, D. Hao, M. Zhu, J. Zhang, *Small Methods* **2023**, *7*, 2300168.
[92] Q. Ke, Q. Xu, X. Lai, M. Li, J. Li, K. Yan, Y. Qiu, *Batteries Supercaps* **2023**, *6*, e202300144.
[93] J. Zhong, Z. Wang, X. Yi, X. Li, H. Guo, W. Peng, J. Wang, G. Yan, *Small* **2024**, *20*, 2308678.
[94] S. Li, W. Zhang, Q. Wu, L. Fan, X. Wang, X. Wang, Z. Shen, Y. He, Y. Lu, *Angew. Chem. Int. Ed.* **2020**, *59*, 14935–14941.
[95] S. F. Liu, X. Ji, N. Piao, J. Chen, N. Eidson, J. J. Xu, P. F. Wang, L. Chen, J. X. Zhang, T. Deng, S. Hou, T. Jin, H. L. Wan, J. R. Li, J. P. Tu, C. S. Wang, *Angew. Chem. Int. Ed.* **2021**, *60*, 3661–3671.
[96] W. Zhang, Q. Wu, J. Huang, L. Fan, Z. Shen, Y. He, Q. Feng, G. Zhu, Y. Lu, *Adv. Mater.* **2020**, *32*, 2001740.
[97] Y. L. Jie, X. J. Liu, Z. W. Lei, S. Y. Wang, Y. W. Chen, F. Y. Huang, R. G. Cao, G. Q. Zhang, S. H. Jiao, *Angew. Chem. Int. Ed.* **2020**, *59*, 3505–3510.
[98] X. Q. Zhang, X. B. Cheng, X. Chen, C. Yan, Q. Zhang, *Adv. Funct. Mater.* **2017**, *27*, 1605989.
[99] N. Piao, S. Liu, B. Zhang, X. Ji, X. Fan, L. Wang, P.-F. Wang, T. Jin, S.-C. Liou, H. Yang, *ACS Energy Lett.* **2021**, *6*, 1839–1848.
[100] D. Lu, R. Li, M. M. Rahman, P. Yu, L. Lv, S. Yang, Y. Huang, C. Sun, S. Zhang, H. Zhang, *Nature* **2024**, *627*, 101–107.
[101] S. Li, Z. Luo, L. Li, J. Hu, G. Zou, H. Hou, X. Ji, *Energy Storage Mater.* **2020**, *32*, 306–319.
[102] H. Zeng, K. Yu, J. Li, M. Yuan, J. Wang, Q. Wang, A. Lai, Y. Jiang, X. Yan, G. Zhang, *ACS Nano* **2024**, *18*, 1969–1981.
[103] X. Y. Zheng, L. Q. Huang, W. Luo, H. T. Wang, Y. M. Dai, X. Y. Liu, Z. Q. Wang, H. H. Zheng, Y. H. Huang, *ACS Energy Lett.* **2021**, *6*, 2054–2063.
[104] T. D. Pham, A. Bin Faheem, K. K. Lee, *Small* **2021**, *17*, 2103375.
[105] D. J. Yoo, S. Yang, K. J. Kim, J. W. Choi, *Angew. Chem. Int. Ed.* **2020**, *59*, 14869–14876.
[106] W. M. Teng, J. X. Wu, Q. H. Liang, J. J. Deng, Y. Xu, Q. Liu, B. Wang, T. Ma, D. Nan, J. Liu, B. H. Li, Q. S. Weng, X. L. Yu, *Energy Environ. Mater.* **2023**, *6*, e12355.
[107] J. Chen, H. Zhang, M. Fang, C. Ke, S. Liu, J. Wang, *ACS Energy Lett.* **2023**, *8*, 1723–1734.
[108] X. Dong, Y. Lin, P. Li, Y. Ma, J. Huang, D. Bin, Y. Wang, Y. Qi, Y. Xia, *Angew. Chem. Int. Ed.* **2019**, *58*, 5623–5627.
[109] J. Liu, B. Yuan, L. Dong, S. Zhong, Y. Ji, Y. Liu, J. Han, C. Yang, W. He, *Batteries Supercaps* **2022**, *5*, e202200256.
[110] H. Yang, Y. Qiao, Z. Chang, P. He, H. Zhou, *Angew. Chem. Int. Ed.* **2021**, *60*, 17726–17734.
[111] X. Liu, A. Mariani, T. Diemant, M. E. Di Pietro, X. Dong, P.-H. Su, A. Mele, S. Passerini, *ACS Energy Lett.* **2024**, *9*, 3049–3057.
[112] G. Zhang, J. Li, S.-S. Chi, J. Wang, Q. Wang, R. Ke, Z. Liu, H. Wang, C. Wang, J. Chang, Y. Deng, J. Lu, *Adv. Funct. Mater.* **2024**, *34*, 2312413.
[113] A. L. Phan, B. Nan, P. M. L. Le, Q. Miao, Z. Wu, K. Le, F. Chen, M. Engelhard, T. Dan Nguyen, K. S. Han, J. Heo, W. Zhang, M. Baek, J. Xu, X. Zhang, P. Liu, L. Ma, C. Wang, *Adv. Mater.* **2024**, *36*, 2406594.
[114] G. Cai, H. Gao, M. Li, V. Gupta, J. Holoubek, T. A. Pascal, P. Liu, Z. Chen, *Angew. Chem. Int. Ed.* **2024**, *63*, e202316786.
[115] C. V. Amanchukwu, Z. Yu, X. Kong, J. Qin, Y. Cui, Z. N. Bao, *J. Am. Chem. Soc.* **2020**, *142*, 7393–7403.
[116] Y. Zhao, T. H. Zhou, T. Ashirov, M. El Kazzi, C. Cancellieri, L. P. H. Jeurgens, J. W. Choi, A. Coskun, *Nat. Commun.* **2022**, *13*, 2575.
[117] Z. Yu, H. S. Wang, X. Kong, W. Huang, Y. C. Tsao, D. G. Mackanic, K. C. Wang, X. C. Wang, W. X. Huang, S. Choudhury, Y. Zheng, C. V. Amanchukwu, S. T. Hung, Y. T. Ma, E. G. Lomeli, J. Qin, Y. Cui, Z. N. Bao, *Nat. Energy* **2020**, *5*, 526–533.
[118] Y. Zhao, T. H. Zhou, M. Mensi, J. W. Choi, A. Coskun, *Nat. Commun.* **2023**, *14*, 299.
[119] J. Shi, C. Xu, J. Lai, Z. Li, Y. Zhang, Y. Liu, K. Ding, Y.-P. Cai, R. Shang, Q. Zheng, *Angew. Chem. Int. Ed.* **2023**, *62*, e202218151.
[120] S. Qi, J. He, J. Liu, H. Wang, M. Wu, F. Li, D. Wu, X. Li, J. Ma, *Adv. Funct. Mater.* **2021**, *31*, 2009013.
[121] P. Bai, J. Li, F. R. Brushett, M. Z. Bazant, *Energy Environ. Sci.* **2016**, *9*, 3221–3229.
[122] S. Li, M. Jiang, Y. Xie, H. Xu, J. Jia, J. Li, *Adv. Mater.* **2018**, *30*, 1706375.
[123] X. Fan, X. Ji, L. Chen, J. Chen, T. Deng, F. Han, J. Yue, N. Piao, R. Wang, X. Zhou, *Nat. Energy* **2019**, *4*, 882–890.
[124] O. Borodin, M. Olguin, P. Ganesh, P. R. Kent, J. L. Allen, W. A. Henderson, *Phys. Chem. Chem. Phys.* **2016**, *18*, 164–175.
[125] Z. Piao, R. Gao, Y. Liu, G. Zhou, H.-M. Cheng, *Adv. Mater.* **2023**, *35*, 2206009.

[126] Q. Sun, Z. Cao, Z. Ma, J. Zhang, H. Cheng, X. Guo, G.-T. Park, Q. Li, E. Xie, L. Cavallo, Y.-K. Sun, J. Ming, *ACS Energy Lett.* **2022**, *7*, 3545–3556.
[127] X.-T. Yang, C. Han, Y.-M. Xie, R. Fang, S. Zheng, J.-H. Tian, X.-M. Lin, H. Zhang, B.-W. Mao, Y. Gu, Y.-H. Wang, J.-F. Li, *Small* **2024**, *20*, 2311393.
[128] Y. Liu, J. Li, X. Deng, S. S. Chi, J. Wang, H. Zeng, Y. Jiang, T. Li, Z. Liu, H. Wang, *Small* **2024**, *20*, 2311812.
[129] S. S. Zhang, T. R. Jow, K. Amine, G. L. Henriksen, *J. Power Sources* **2002**, *107*, 18–23.
[130] M. Ue, *J. Electrochem. Soc.* **1994**, *141*, 3336.
[131] H. K. Bergstrom, B. D. McCloskey, *ACS Energy Lett.* **2024**, *9*, 373–380.
[132] K. M. Diederichsen, E. J. McShane, B. D. McCloskey, *ACS Energy Lett.* **2017**, *2*, 2563–2575.
[133] A. Jana, S. I. Woo, K. Vikrant, R. E. García, *Energy Environ. Sci.* **2019**, *12*, 3595–3607.
[134] Y. Watanabe, Y. Ugata, K. Ueno, M. Watanabe, K. Dokko, *Phys. Chem. Chem. Phys.* **2023**, *25*, 3092–3099.
[135] L. Suo, Y.-S. Hu, H. Li, M. Armand, L. Chen, *Nat. Commun.* **2013**, *4*, 1481.

Manuscript received: April 25, 2024
Revised manuscript received: September 14, 2024
Accepted manuscript online: September 19, 2024
Version of record online: October 31, 2024